

## Electronic Supplementary Information

### Unravelling “off-target” effects of redox-active polymers and polymer multilayered capsules in prostate cancer cells

Giovanni L. Beretta,<sup>a,†</sup> Marco Folini,<sup>a,†</sup> Francesca Cavalieri,<sup>b,c</sup> Yan Yan,<sup>c</sup> Enrico Fresch,<sup>b</sup> Subramanian Kaliappan,<sup>b</sup> Christoph Hasenöhr,<sup>d</sup> Joseph J. Richardson,<sup>c</sup> Stella Tinelli,<sup>a</sup> Andreas Fery,<sup>d</sup> Frank Caruso,<sup>c,\*</sup> Nadia Zaffaroni<sup>a,\*</sup>

<sup>a</sup>Department of Experimental Oncology and Molecular Medicine, Fondazione IRCCS Istituto Nazionale dei Tumori, Via G. Amadeo 42, 20133 Milan, Italy. Email: [nadia.zaffaroni@istitutotumori.mi.it](mailto:nadia.zaffaroni@istitutotumori.mi.it)

<sup>b</sup>Dipartimento di Scienze e Tecnologie Chimiche, Università di Roma Tor Vergata, 00173 Roma, Italy.

<sup>c</sup>ARC Centre of Excellence in Convergent Bio-Nano Science and Technology, and the Department of Chemical and Biomolecular Engineering, The University of Melbourne, Parkville, Victoria 3010. Australia. Email:

[fcaruso@unimelb.edu.au](mailto:fcaruso@unimelb.edu.au)

<sup>d</sup>Department of Physical Chemistry II, University of Bayreuth, Bayreuth 95440, Germany

<sup>†</sup>these authors contributed equally.

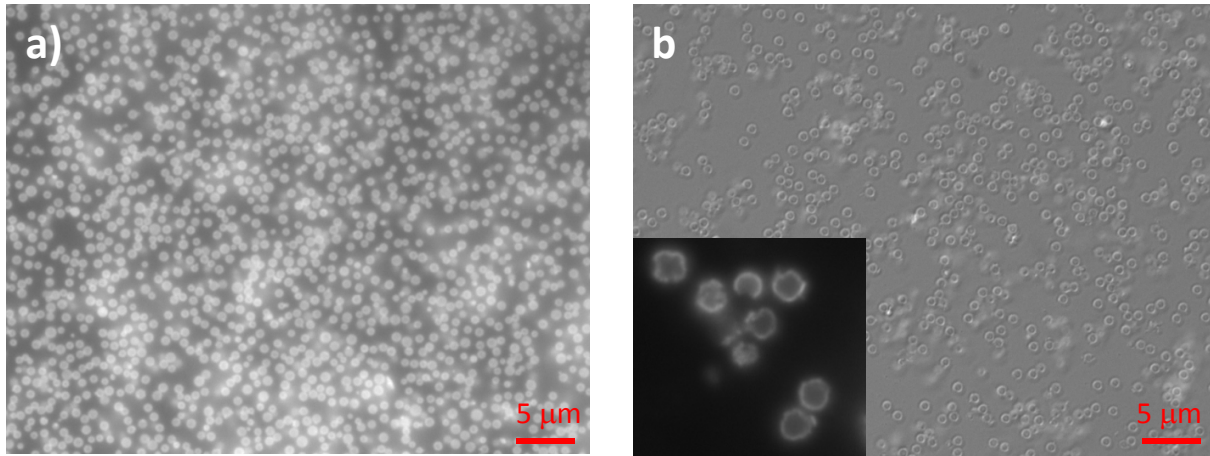


**Fig. S1.** Representative microscopy images showing a) pHPMASh  $\mu$ C loaded with AF488-PLL; b) DIC microscopy image of intact pHPMASh  $\mu$ C and broken  $\mu$ C after 0.5 M DTT 1 h treatment (inset).

**Table S1. Structural properties of PMA<sub>SH</sub> and pHPMASh  $\mu$ Cs**

	pHPMASH $\mu$ Cs	PMA <sub>SH</sub> $\mu$ Cs
Thickness [ $\mu$ m]	$31 \pm 3$	$10 \pm 6$
Stiffness [mN/m]	$6 \pm 3$	$7 \pm 3$

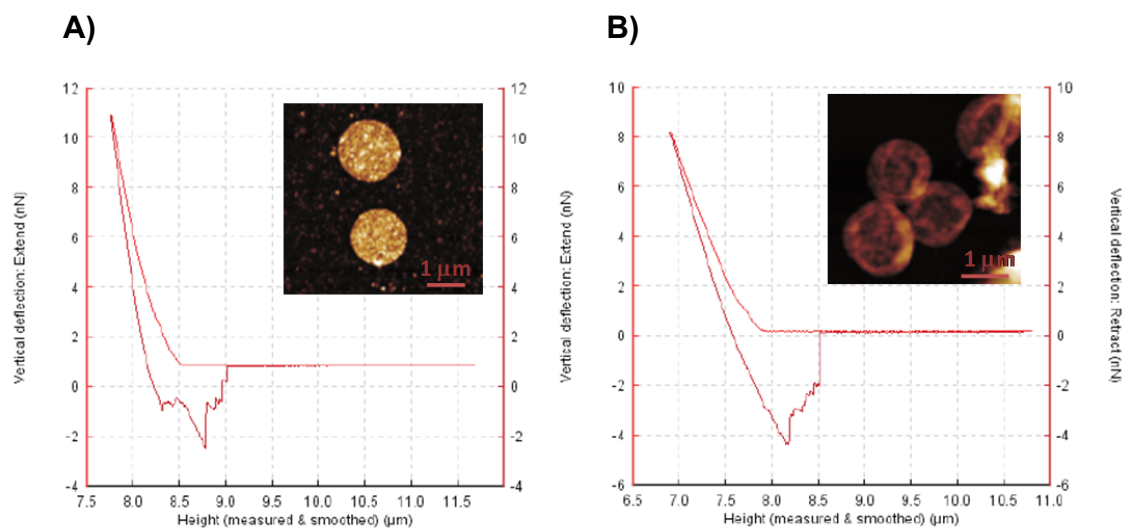


**Fig S2.** Representative force curves acquired on A) PMA<sub>SH</sub> μCs and B) pHPMA<sub>SH</sub> μCs. Insets show AFM scans of μCs dried and immobilized onto a PEI-treated substrate.

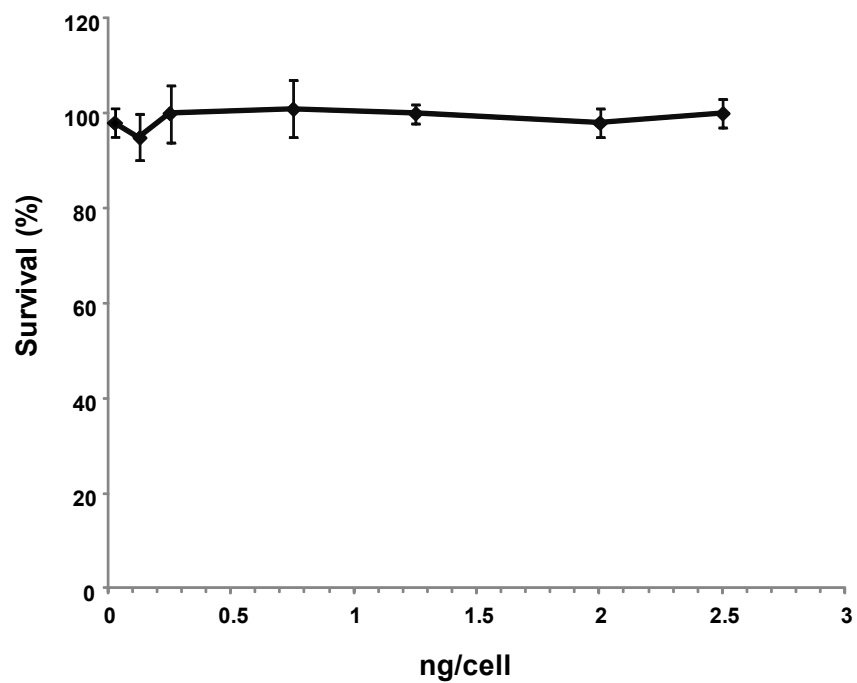
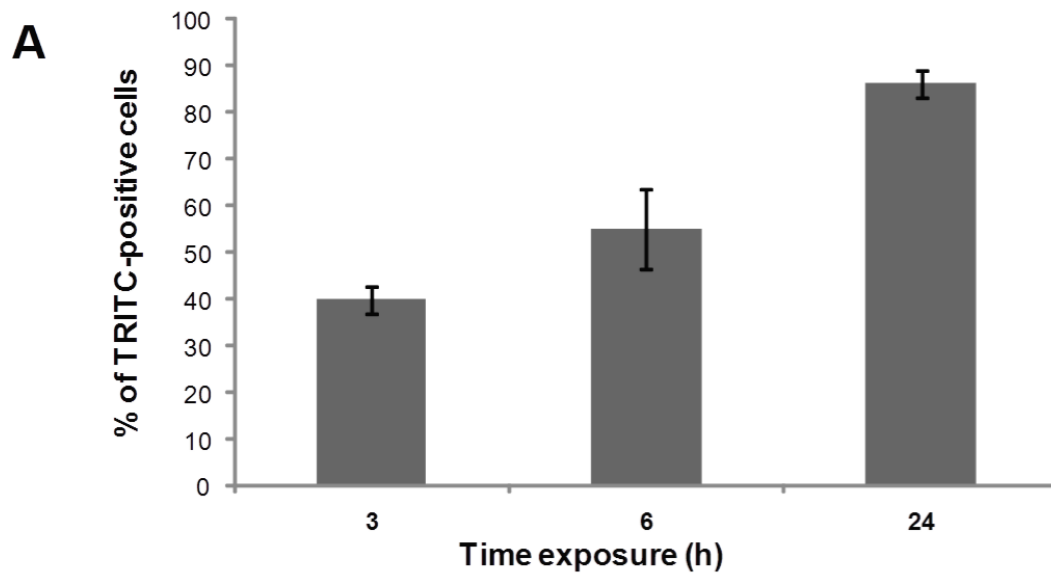


**Fig. S3.** DU145 cell survival curves after 120 h exposure to PMA<sub>SH</sub> polymer. Data are reported as a percentage of viable cells exposed to polymer compared with untreated cells. All data represent mean values  $\pm$  SD.



**B**

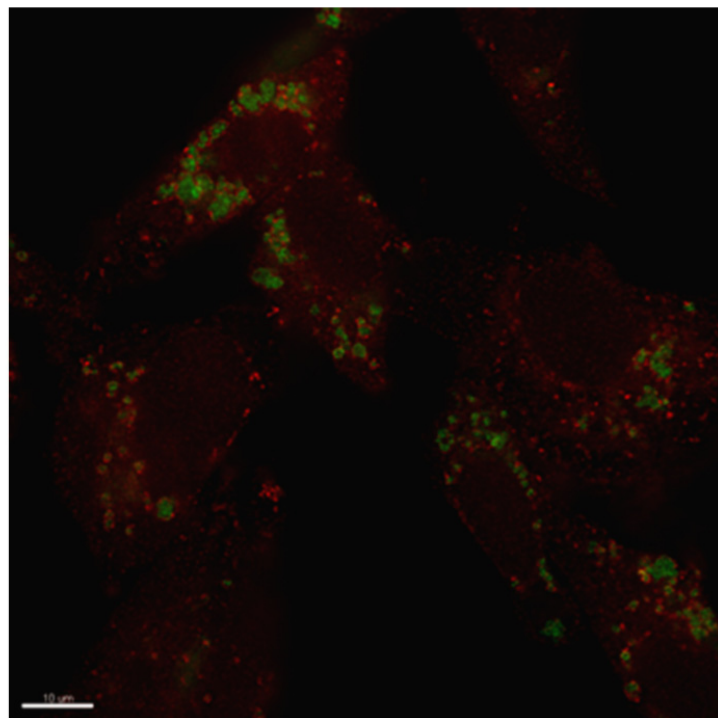


**Fig. S4.** Cellular uptake and distribution of pHPMA<sub>SH</sub>  $\mu$ Cs in PC-3 cells. A) The time-dependent uptake of AF647-labeled pHPMA<sub>SH</sub>  $\mu$ Cs was analyzed by flow cytometry. PC-3 cells were exposed to capsules at a capsule/cell ratio of 72:1. B) Representative deconvolution microscopy images showing the localization of AF488-labeled pHPMA<sub>SH</sub>  $\mu$ Cs (green) in PC-3 cells after 24 h exposure to a capsule/cell ratio of 500:1. Lysosomes are visualized after staining for the LAMP1 marker using an AF647 secondary antibody (red).

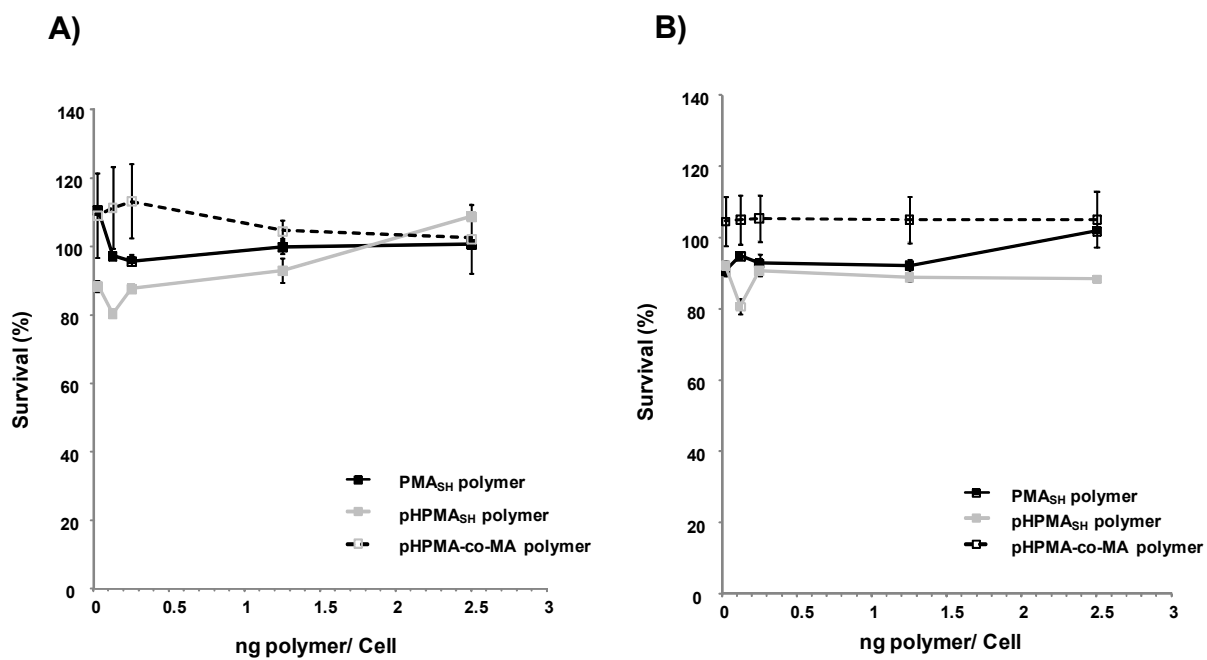


**Fig. S5.** A) PC-3 and B) DU145 cell survival curves after 96 h exposure to pHPMA-co-MA, pHPMA<sub>SS</sub> with 15% thiol moieties, and PMA<sub>SS</sub> polymer with 15% thiols groups. Data are reported as a percentage of viable cells exposed to polymers compared with untreated cells. All data represent mean values  $\pm$  SD.

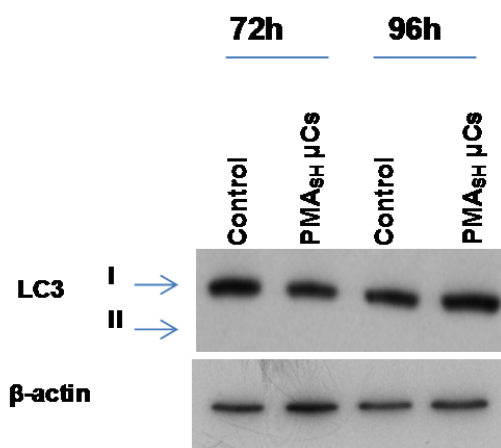


**Fig. S6.** Representative Western immunoblotting showing LC3-I and II expression levels in DU145 cells exposed for 72 h and 96 h to PMA<sub>SH</sub> μCs (125 μCs/cell). β-actin was used as control for equal protein loading.

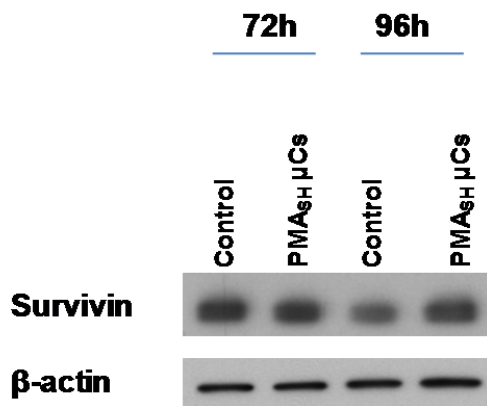


**Fig. S7.** Representative Western immunoblotting showing survivin expression levels in DU145 cells exposed for 72 h and 96 h to PMA<sub>SH</sub> μCs (125 μCs/cell). β-actin was used as control for equal protein loading.